Dalton Transactions

Accepted Manuscript

ROYAL SOCIETY OF CHEMISTRY

www.rsc.org/dalton

Semiconducting Composite Oxide Y_2CuO_4-5CuO Thin Films for Investigation of Photoelectrochemical Properties†

Sohail Ahmed,[a] Muhammad Adil Mansoor,[a] Muhammad Mazhar,*[a] Tilo Söhnel,[b,c] Hamid Khaledi,[a] Wan Jefrey Basirun,[d] Zainudin Arifin,[a] Shahzad Abubakar[e] and Bakhtiar Muhammad[f]

ABSTRACT

An octa-nuclear heterobimetallic complex $[Y_2Cu_6Cl_{0.7}(dmae)_6(OAc)_{7.3}(OH)_4(H_2O)_2].3H_2O.0.3CH_3C_6H_5$ **1** (dmae = dimethylaminoethanoate; OAc = acetato) was synthesized and characterized by melting point, elemental analysis, FT–IR, single crystal X-ray diffraction analysis and implemented at 600 ^oC under oxygen atmosphere for the deposition of Y_2CuO_4–5CuO composite thin films by aerosol assisted chemical vapor deposition (AACVD). The chemical composition and surface morphology of the deposited thin film have been determined by X-ray diffraction, scanning electron microscopy and energy dispersive X-ray analysis that suggest the formation of impurity-free crystallite mixtures of Y_2CuO_4–5CuO composite, with well-defined evenly distributed particles in the size range of 19-24 nm. The optical band gap energy of 1.82 eV was estimated by UV-visible spectrophotometery. PEC studies show that under illumination with 150 W halogen lamp and at potential of 0.8 V, a photocurrent density of 9.85 μAcm^{-2} was observed.

Keywords: Heterobimetallic Complex, Copper-Yttrium Composite Oxide, Thin Films, Band gap, PEC studies.

[a] *Department of Chemistry, Faculty of Science, University of Malaya, Kuala Lumpur 50603, Malaysia. Phone :+60379674269 Email: mazhar42pk@yahoo.com*

[b] *School of Chemical Sciences, The University of Auckland, Private Bag 92019, Auckland, New Zealand*

[c] *Centre for Theoretical Chemistry and Physics, The New Zealand Institute for Advanced Study, Massey University Auckland, New Zealand*

[d] *Institute of Nanotechnology and Catalysis (NanoCat), Institute of Postgraduate Studies, University of Malaya, 50603, Kuala Lumpur, Malaysia.*

[e] *NS&CD, National Centre for Physics, Quaid-I-Azam University, Islamabad 44000, Pakistan*

[f] *Department of Chemistry, Hazara University, Mansehra, KPK, Pakistan.*

† Electronic supplementary data (ESI) available. CCDC 950391

1. Introduction

Highly crystalline bi- and tri-metallic ceramic oxides constitute an important class of materials that have found a wide range of advanced applications such as superconductors, structural ceramics, sensors, catalysts and actuators in addition to their use in ferroelectric and dielectric materials for microelectronic data processing devices.[1-3] Several methods[4-8] with their own merits and demerits are available for thin film fabrication, but the use of single source precursor in chemical vapour deposition (CVD) is gaining more attention because it provides advantages of excellent film uniformity, high deposition rates, control over material composition and phase, conformal coverage on complex geometries, controllability of film microstructures, low-cost and scalability. An easily adaptable sub-branch of CVD known as aerosol assisted chemical vapour deposition (AACVD) provides an attractive method to deposit metal oxide thin films.[9-14] The keen interest towards the synthesis of mixed yttrium, barium and copper heterotrimetallic complexes is to possibly fabricate the high temperature 1-2-3 superconductor $YBa_2Cu_3O_{7-x}$ from a single source and further transform it into useful forms such as films, wires and fibers.[15] These hetero-bimetallic complexes may not only model as the intermediate species, but may also find direct application as precursors for the synthesis of high T_c superconductors. Although extensive work has been done on the development of heterometallic complexes of copper with yttrium and barium such as $[Y_2Cu_8(\mu\text{-}PyO)_{12}(\mu\text{-}Cl)_2(\mu_4\text{-}O)_2(NO_3)_4(H_2O)_2.2H_2O]$,[15] $[Ba\{Cu[OCMe(CF_3)_2]_3\}]$,[16] $[Y_2Cu_8O_2(PyO)_{12}Cl_2(NO_3)_4(H_2O)_2]$,[17] $\{[Ba_3Cu_2(CF_3CO_2)_6(Me_2NC_2H_4O)_4(MeOH)_2]_2MeOH\}$,[18] $[BaCu_4(PyO)_4(bdmap)_4(O_2CCF_3)_2]$, $[BaCu_4(PyO)_4(deae)_4(O_2CCF_3)_2]$,[19] $[BaCu(C_2H_6O_2)_6(C_2H_4O_2)_2]$ and $[BaCu(C_2H_6O_2)_3(C_2H_4O_2)_2]$,[20] but none of these compounds have been investigated for their implementation as a precursor for chemical vapour deposition of Y-Cu ceramic oxides. In continuation of our efforts directed towards the development of bi- and trimetallic complexes,[21,22] we focussed our attention on the use of multifunctional ligands, such as aminoalkoxides and acetate as a tool to strengthen the interaction between the components of heterobimetallic species. We utilized tetrameric $[Cu(dmae)Cl]_4$ complex, for the preparation of heterobimetallic complex in which 2-dimethylaminoethanol (dmae) serves as a bridging ligand to coordinate copper and yttrium and also impart coordinative saturation and enhance the volatility and solubility of the complex, which is of utmost importance for AACVD. Hence, we synthesized the heterobimetallic complex $[Y_2Cu_6Cl_{0.7}(dmae)_6(OAc)_{7.3}(OH)_4(H_2O)_2].3H_2O.0.3CH_3C_6H_5$ **1** and used it as a precursor for the growth of impurity-free Y_2CuO_4–5CuO composite thin films using AACVD technique at 600 °C. The deposited films were characterized by XRPD, SEM, EDX and UV-visible spectrophotometry for their stoichiometry, morphology, thickness and optical band gap. Further scope of these thin films for the application in harvesting sunlight for photoelectrochemical water splitting to hydrogen and oxygen is also investigated.

2. Experimental

2.1. Material and methods

All experiments were carried out under an inert atmosphere of dry argon gas using Schlenk tube and glove box techniques. All solvents were purchased from Fluka chemical company. Toluene was rigorously dried over sodium benzophenoate and methanol was purified by distilling over reagent grade magnesium powder. *N*,*N*-dimethylaminoethanol (dmaeH) was purchased from Aldrich, purified by refluxing over K_2CO_3 for 10 h and distilled immediately before use. The melting point was determined in a capillary tube using an electrothermal melting point apparatus, model MP.D Mitamura Riken Kogyo (Japan) and is uncorrected. The microanalyses were performed using a Leco CHNS 932. FT-IR spectra were recorded on a single reflectance ATR instrument (4000–400 cm^{-1}, resolution 4 cm^{-1}). The controlled thermal analysis was investigated using a Mettler Toledo TGA/ SDTA 851e Thermogravimetric Analyzer with a computer

interface. The thermal measurements were carried out in an alumina crucible under an atmosphere of flowing nitrogen gas (50 cm^3 min^{-1}) with a heating rate of 20 ^oC min^{-1}.

2.2. Synthesis of $[Y_2Cu_6Cl_{0.7}(dmae)_6(OAc)_{7.3}(OH)_4(H_2O)_2].3H_2O.0.3CH_3C_6H_5$ 1

0.70 g (0.1mol) freshly cut lithium metal dissolved in 15 mL dry methanol was added slowly to a solution of 6.72 g (0.05 mol) $CuCl_2$ dissolved in 50 mL of methanol in a Schlenk tube fitted with vacuum/Ar gas line and magnetic stirrer. The reaction mixture was stirred for 8 hours and allowed to stand for three hours, filtered through cannula and dried under vacuum. 5 mL (0.05 mol) dmaeH was injected drop wise through the rubber septum and the contents were stirred for 3 hours the excess of unreacted dmaeH was subsequently removed under vacuum. At this stage 13.56 g $Y(OAc)_3.xH_2O$ suspended in 25 mL of toluene was added drop wise with vigorous stirring that continued overnight. Filtration through a cannula gave a clear light blue solution that was evaporated to dryness under vacuum. The solid was washed three time with 5 mL dry n-hexane and re-dissolved in 3 mL of toluene to yield light blue crystals m.p 137 ^oC after 20 days at -10 ^0C.

The stoichiometry of the complex has been determined by microanalysis (CHN), FT-IR, thermogravimetry and single crystal X-ray diffraction analysis. Elemental analysis for $[Y_2Cu_6Cl_{0.7}(dmae)_6(OAc)_{7.3}(OH)_4(H_2O)_2].3H_2O.0.3CH_3C_6H_5$ **1**: Calculated (found) **%** C, 28.3 (28.8); H, 5.7 (6.0); N, 4.9 (5.4), FT–IR (cm^{-1}): 2976(w), 2868(m), 1571s, 1415s, 1385s, 1333w, 1271m, 1079 (m), 1026(m), 512 (m), 464 (w). TGA: 50-62 °C (1.9 wt % loss), 62-105 °C (9.9 wt % loss), 105-195°C (15.2 wt % loss), 195-232 °C (38 wt % loss), 232-348 °C (57 wt % loss), 348-404 °C (60.27 wt % loss) Residue = 39.73 %:Calc. = 38 %).

2.3 Single-crystal X-ray crystallography

Single crystal XRD measurements were performed on a CCD diffractometer (Bruker Smart APEXII) with graphite-monochromatized Mo$K\alpha$ radiation, λ_{Mo} = 0.71073 Å. Data reduction was carried out using the SAINT[23] program. Semi-empirical absorption corrections were applied based on equivalent reflections using SADABS[24]. The structure solution and refinements were performed with the SHELXL-2013 program package[25]. All the non-hydrogen atoms were refined anisotropically and all the C-bound hydrogen atoms were placed at calculated positions and refined isotropically. O-bound hydrogen atoms were located in difference Fourier maps and refined with distance restraint of O–H 0.84(2) Å. The Cl atom has substitutional disorder with acetate with an occupancy ratio of 0.7:0.3. Crystal data: $C_{40.70}H_{98.30}Cl_{0.7}Cu_6N_6O_{29.60}Y_2$, blue prism, 0.14 × 0.12 × 0.10 mm^3, monoclinic, $P\ 2_1/c$, a = 22,3199(9), b = 13.7789(6), c = 23.233(1) Å, β = 105.863(3)°, V = 6873.1(5) $Å^3$, Z = 4; 113043 unique data (R_{int} = 0.1033), 12795 reflections, 8979 reflections observed [$(I > 2\sigma(I)]$, final R indices [$(I > 2\sigma(I)]$ R_1 = 0.0393, wR_2 = 0.0787.

2.3. Deposition of thin films by AACVD

The thin films were deposited on commercially available FTO-coated glass substrates using self-designed AACVD assembly as described elsewhere.[26] FTO-coated glass substrates of size 2 x 1 cm (L x W) purchased from Sigma Aldrich were

cleaned by ultrasonic washing with distilled water, acetone, and ethyl alcohol prior to their use. Finally, they were washed with distilled water, stored in ethanol and dried in air. Substrate slides were placed inside the reactor tube and then heated up to the deposition temperature for 10 min before carrying out the deposition. The aerosol of the precursor solution was formed by keeping the round bottom flask in a water bath above the piezoelectric modulator of an ultrasonic humidifier. The generated aerosol droplets of the precursor were transferred into the hot wall zone of the reactor by compress air. At the end of the deposition, the aerosol line was closed and only carrier gas passed over the substrate to cool to room temperature before it was taken out from the reactor**.** In a typical experiment, 50 mg of the precursor **1** was dissolved in 30 mL of toluene to deposit thin films of composite Y_2CuO_4-5CuO on FTO-conducting glass under compressed air with a flow rate of 150 cm^3 min^{-1} at 600 ^oC. The deposited thin films are light yellow in colour, transparent, uniform, robust, and stable towards atmospheric conditions and adhere strongly on FTO substrate as verified by the "scotch tape test**"**.[27]

2.3.1. Characterisation of thin films

The surface morphology of thin films was studied using a field-emission gun scanning electron microscope (FESEM, FEI Quanta 400) coupled with Energy Dispersive X-ray spectrometer EDX (INCA Energy 200 (Oxford Inst.)), at an accelerating voltage of 10 kV, and a working distance of 6mm. The final products were characterised using X-ray powder diffraction (XRD) on a D8 Advance X-Ray Diffractometer (Bruker AXS) using Cu*Kα* radiation (λ=1.540 Å), at a voltage of 40 kV and current of 40 mA at ambient temperature. The optical absorption spectrum of the thin films having thickness of 310 nm as measured by profilometer KLA Tencore P-6 surface profiler was recorded on a Lambda 35 Perkin-Elmer UV-visible spectrophotometer in the wavelength range of 350-850 nm.

The photo-electrochemical response of fabricated Y_2CuO_4–5CuO layers was studied by electrochemical techniques such as linear scanning voltammetry (LSV) in the absence and presence of light (150 W halogen lamp). A three-compartment cell with a saturated calomel electrode (SCE) as the reference electrode (RE) and Y_2CuO_4–5CuO /FTO (0.5 × 1× 1 cm) as the working electrode, and Pt wire as a counter electrode was used for the photocurrent measurements. General purpose electrochemical software (GPES) was used in the linear scan voltammetry (LSV) by Autolab PGSTAT-302N. The scan rate for LSV was 25 mV s^{-1} between 0 V to 0.8 V.

3. Results and discussion

3.1. Synthesis and characterization

Tetrameric complex $[Cu(dmae)Cl]_4$ reacts quantitatively with $Y(acetate).XH_2O$ in toluene solution to yield complex 1[28] (m.p = 137 ^oC) as shown in chemical equation 1.

$$3/2[Cu((CH_3)_2NCH_2CH_2O)Cl]_4 + 3Y(CH_3COO)_3.\,xH_2O \xrightarrow{\text{Toluene}} [Y_2Cu_6Cl_{0.7}((CH_3)_2NCH_2CH_2O)_6(CH_3COO)_{7.3}(OH)_4(H_2O)_2].3H_2O.0.3CH_3C_6H_5 + Y(OH)_3 + 1.7CH_3COOH + 5.3HCl \quad (1)$$

The complex **1** is soluble in common organic solvents such as dichloromethane, chloroform and tetrahydrofuran and is stable in air under normal conditions. The structure and stoichiometry of the complex was ascertained by the single crystal analysis, micro-analysis and FT-IR that revealed formation of Y-Cu bimetallic complex in which two Y and six Cu atoms are bridged through oxygen

atoms of acetato and dimethylaminoethanolato ligands in addition to four hydroxo groups. The use of multifunctional ligands coordinatively saturates each metal atom and restricts its ability to oligomerize at the same time enhancing its solubility in organic solvents and making it useful as a precursor to fabricate bimetallic composite oxide thin films. In the FT–IR spectrum, an absorption band at 3295 cm^{-1} is due to water molecules; the presence of both carboxylate and aminoalcoholate ligands in the complex were also identified by their vibration signals. The two strong absorption bands between 1400 and 1700 cm^{-1} for the carboxylate group suggest a dominant chelating or bridging–chelating behaviour for the acetate ligands. The anti-symmetric and symmetric stretching vibrations for CO_2 were assigned at 1571 cm^{-1} and 1415 cm^{-1}, respectively[29]. The difference of 156 cm^{-1} between the anti-symmetric and symmetric stretching vibrations suggests a chelating or bridging–chelating behaviour for carboxylate ligands[30,31]. The presence of three strong absorption bands in the range of 1120-1270 cm^{-1} for ν(C–O) stretching corresponds to carboxylate ligands[29]. The absorptions at the low frequencies of 512 and 464 cm^{-1} are probably due to M–O and M–N stretching vibrations, respectively (Fig. S1)[32].

3.2. Structural analysis of $[Y_2Cu_6Cl_{0.7}(dmae)_6(OAc)_{7.3}(OH)_4(H_2O)_2].3H_2O.0.3\ CH_3C_6H_5$ 1

A schematic drawing of the Y-Cu complex is shown in Fig. 1a and the crystal structure is depicted in Fig. 1b-d. The structure consists of discrete heterometallic complexes cocrystallized with a partially occupying toluene and three water molecules. The metal complex molecule contains two Y^{3+} and six Cu^{2+} metal centres. Each Y^{3+} atom is eight-fold coordinated in a dodecahedral geometry by three μ_3-OH^-, three μ_2-O_{dmae} and one bidentate acetate group with Y-O distances ranging between 2.250(3) and 2.503(3) Å. Each Cu^{2+} center is five-fold coordinated in a square-pyramidal geometry by an *N,O*-bidentate chelate of dmae, one μ_3-OH^- and one bridging acetate O atom. The fifth ligand in three of the copper centers (Cu2, Cu3 and Cu5) is an equatorially placed monodentate acetate group and in two centers (Cu1 and Cu4) is an apically bound water molecule. In case of Cu6, the fifth ligand is a Cl ligand in the equatorial plane, which is partially replaced by a monodentate acetate group.

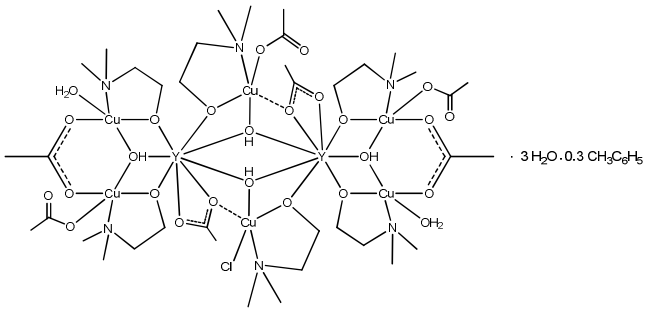

Fig. 1a Schematic diagram of $[Y_2Cu_6\ Cl_{0.7}\ (dmae)_6(OAc)_{7.3}\ (OH)_4(H_2O)_2].3H_2O.0.3\ CH_3C_6H_5$, **1**

The eight metal centers in the structure are O-bridged into a $Y_2Cu_6O_{12}$ cluster (Fig. 1c) wherein the bridged metals are separated by a Y-Y distance of 3.8342(7) Å and Y-Cu distances of 3.3093(7)-3.6182(7) Å (Table S1). These values are comparable to those observed in some other Y-Cu complexes[33,34]. Four molecules of **1** are placed in the unit cell (Figure 1d). The Y-Cu complex molecules are connected *via* hydrogen bonding to water solvent clusters $(H_2O)_3$ forming a two-dimensional network parallel to the (*bc)* plane (Fig. S2). The toluene molecules are placed in the cavities between these layers. There is

no significant intermolecular hydrogen bonding interactions between the metal complex molecules.

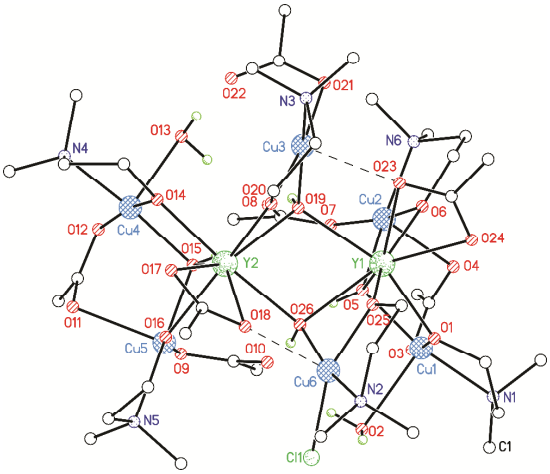

Fig. 1b The molecular structure of **1**. C-bound hydrogen atoms and the solvent molecules are omitted for clarity.

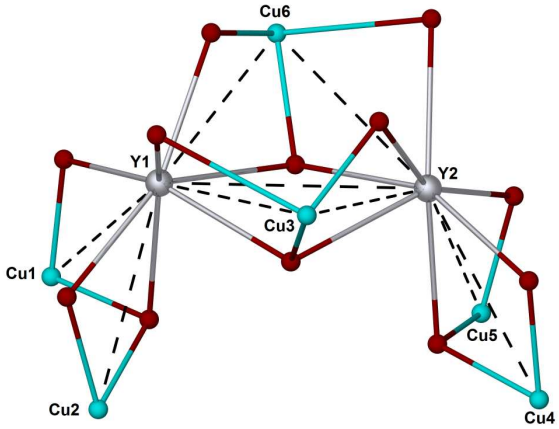

Fig. 1c $Y_2Cu_6O_{12}$ core of the structure of **1**. The red circles represent the bridging O atoms and the black dashed lines represent the metal-metal contacts.

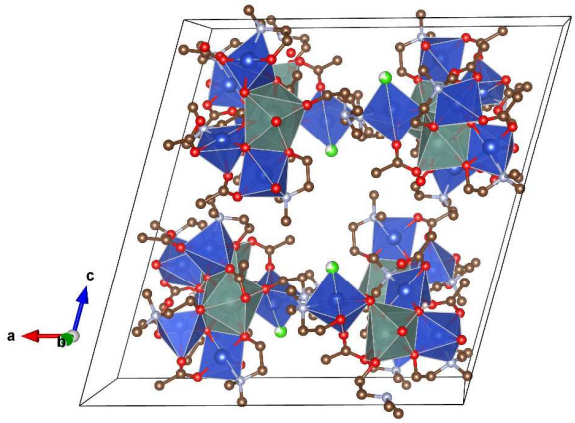

Fig. 1d Approximate content of a unit cell showing four complete Y_2Cu_6 cores of **1**. Hydrogen atoms, solvent molecules and the partial occupied actetate molecules are omitted for clarity.

3.3 Thermal studies of complex 1

The thermal behaviour of **1** has been examined by thermo gravimetric and derivative thermo gravimetric (TGA/DTG) analyses performed under an oxygen and inert nitrogen ambient of flowing gases at 25 cm^3/min at a heating rate of 20 ^oC/min. The DTG (Fig. 2) curve indicates that the initial decomposition steps of complex **1** in both the ambient of oxygen and nitrogen are very similar except that all the main heat intake steps appear late by about 10 ^oC in nitrogen as compared to oxygen atmosphere. DTG curves indicate systematic five distinct stages of heat gain at 76, 120, 222, 336 and at 505 ^oC giving a weight losses of 2.4, 8.7, 36.8, 51.5 and 58.1 % respectively in oxygen ambient, where as in nitrogen atmosphere mass losses occurs at 62, 105, 195, 232 and 348 ^oC yielding a mass losses of 1.9, 9.9, 15.2, 38 and 57 % respectively. In oxygen atmosphere the final pyrolysis step occurs at 466 ^oC where a slight gain in weight along with change in phase takes place to give stable residual mass of 41.9% at 505 ^oC from

complete decomposition of complex **1**. Further heating of the residue to 600 °C did not bring any change in mass loss indicating formation of stable Y_2CuO_4–5CuO composite. FT-IR of the residue obtained from decomposition of complex **1** under oxygen ambient (Fig. S3a) shows absorptions at 630 cm^{-1} and 528 and 557 cm^{-1} confirming presence of Cu-O[35,36] and Y_2O_3[37] respectively. The thermogram recorded in nitrogen atmosphere shows a loss of 57 % of total mass of the complex **1** at 348 °C. Further heating of the sample to 600 °C shows a gradual mass loss indicating incomplete decomposition of the complex **1** at this temperature. This observation has also been affirmed by FT-IR of the residue, that showed strong absorptions band in the region of 3300-3500 cm^{-1} and at 1470 cm^{-1} respectively (Fig. S3b), indicating presence of nitrogenous and carbonaceous impurities in the residue. The total mass loss of complex **1** in nitrogen atmosphere is more than in oxygen atmosphere. It is alleged that under nitrogen atmosphere loss in weight is taking place through β-hydrogen abstraction followed by reductive elimination that reduces most of the Cu(II) to Cu(I) and Cu(0) triggering reduction in weight as confirmed from FTIR of the residue showing absorption at 862 cm^{-1} due to Cu_2O[38] and has also been reported earlier[39]. On the other hand pyrolysis of complex 1under oxidizing atmosphere of oxygen preserves +2 oxidation state of Cu while at the same time oxidizing any nitrogenous and carbonaceous impurities from the ligands to form pureY_2CuO_4-5CuO composite. This observation has been confirmed by XRPD of thin films formed under the similar conditions as indicated in section 3.4 (Fig. 3).

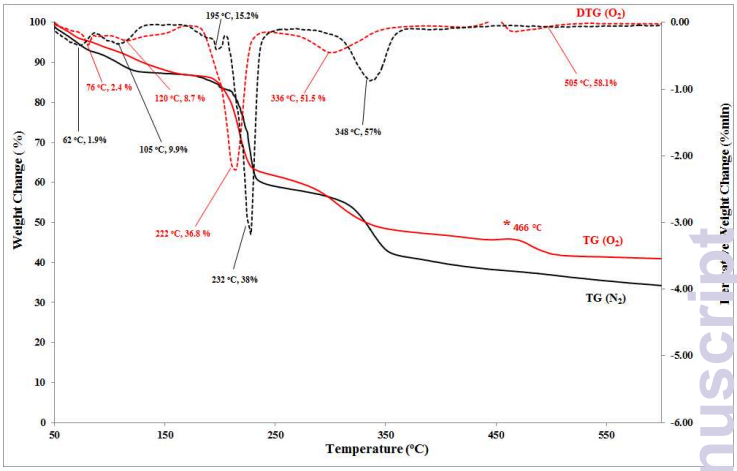

Fig. 2. TGA/DTG curves recorded under oxygen (red) and inert nitrogen (black) ambient showing pyrolysis of complex **1** at gas flow rate of 25 cm^3/min and heating rate of 20 °C/min.

3.4. Powder X-ray diffraction studies of thin films

The powder diffraction pattern Fig. 3 of composite Y_2CuO_4-5CuO thin films deposited on FTO matches very well with ICDD standard card no. [00-046-0622] and [00-002-1040] for tetragonal phase of Y_2CuO_4 and monoclinic phase of CuO respectively. The stick pattern matching is available in the supplementary information (Fig. S4). The relative peak intensities and the position of the diffraction peaks of the Y_2CuO_4-5CuO composite thin films match with Tenorite phase of CuO that crystallizes in monoclinic structure, space group *C*2/*c* with *a* = 4.6530 Å, b =3.4100 Å, c = 5.1080 and β = 99.48°. The Y_2CuO_4 crystallizes in tetragonal structure with space group *I*4/*mmm* resulting in a larger unit cell with lattice parameters of *a* = 3.860 and *c* = 11.7000 Å. In the XRD, peaks at 2θ values of 26.41°, 33.70°, 37.70°, 51.59°, and 64.50° correspond respectively to (110), (101), (200), (211), and (310) lattice reflection planes of SnO_2 (substrate), peaks at 2θ values of 35.46°, 38.70°, 48.81°, 54.74°, 58.22°, 61.72°, 65.74°

and 66.54° correspond respectively to (002), (111), (-202), (020), (-113), (022), and (113) lattice reflection planes of the monoclinic CuO phase whereas peaks at 2θ values of 32.57°, 46.19°, 58.22° and 65.02° correspond respectively to (103), (200), (116) and (220) lattice reflection planes of the tetragonal Y_2CuO_4 phase. The XRD pattern of the thin film indicates dominant phases of FTO and monoclinic CuO whereas tetragonal Y_2CuO_4 gives weak signals possibly due to low deposition temperature of 600 °C where most of this phase remains in amorphous form. The particle size of 38.6 nm has been estimated as calculated from Scherer's equation.

The EDX spectrum (Fig. S5a and Fig. S5b) confirmed the presence of Cu, Y and O elements in the deposited films. The silicon, tin and calcium signals appear from the FTO substrate. The Y: Cu in the films is 0.90: 3, which is in agreement with the expected elemental ratio of 1: 3 present in complex **1**.

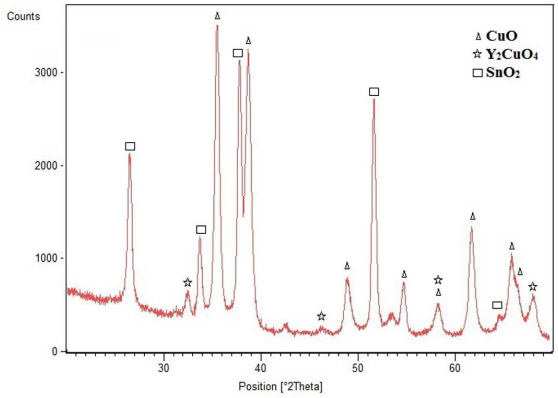

Fig. 3 Powder X-ray diffraction (XRD) pattern of Y_2CuO_4-5CuO composite thin films deposited from precursor **1** at 600 °C in ambient of oxygen for 45 minutes.

3.5. Surface morphology and film thickness

The surface morphology of composite Y_2CuO_4–5CuO thin films grown on FTO glass substrates is presented in Fig. 4. The films deposited at 600 °C comprise of spherical particles in grain size range from 19-24 nm scattered evenly with small void spaces. The particle size of 38.6 nm calculated from XRD peak at 2 theta of 32.57° agrees well with that determined from SEM image.

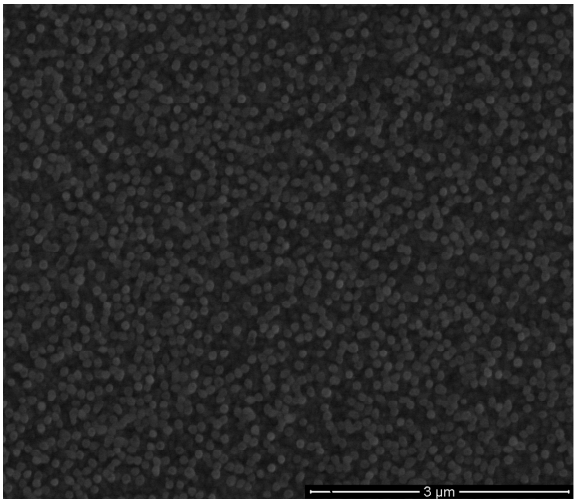

Fig. 4 SEM image of thin film of Y_2CuO_4–5CuO deposited from **1** at 600 °C in an ambient of oxygen for 45 minutes showing spherical granules.

3.6. Optical band gaps

The optical absorption spectrum of thin films was recorded in the wavelength range of 350-850 nm using similar FTO coated glass substrate as a reference to exclude the substrate contribution in the spectrum. The UV-visible spectrum of Y_2CuO_4–5CuO composite thin film shows wide range absorption which gradually increases towards lower wavelength and shows maximum absorption in the range of 540 – 375 nm. The film shows an indirect optical band gap of band energy of 1.82 eV as calculated from the Tauc plot[40] of energy versus $(\alpha h\upsilon)^2$ (Fig. 5). It is reported that the optical band gap

of CuO falls in the range of 1.2-1.5 eV, [41,42] but we could not find any literature reference regarding optical band gap of either Y_2CuO_4 or composite of Y_2CuO_4-5CuO thin films. Our reported band gap value of 1.82 eV for Y_2CuO_4- 5CuO composite suggests a slight increase in the band gap of CuO by the addition of yttrium to it. This observation is in accordance with the known fact that band gap is seriously affected by the addition of dopants and composite formation[43].

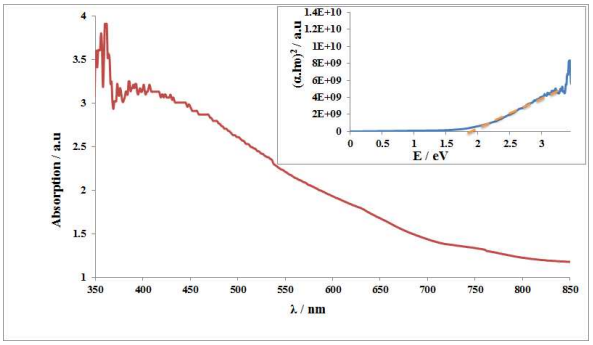

Fig. 5 UV-visible absorption spectrum of wavelength versus absorption and inset Tauc plot of energy versus $(\alpha h\upsilon)^2$ of Y_2CuO_4–5CuO thin films deposited from precursor **1** using AACVD showing a wide range absorption with band gap of 1.82 eV.

3.7. Photoelectrochemical studies

Fig. 6 shows current–voltage characteristics under a dark and simulated sunlight in 0.01 M phosphate buffer (NaH_2PO_4 and Na_2HPO_4) for the Y_2CuO_4–5CuO electrode deposited using the optimum condition of deposition temperature of 600 ^oC, deposition time of 45 min, and 0.0026 M solution of **1** in toluene. The photocurrent density at 0.8V vs. SCE is about 9.85 which is higher than 7.5 μAcm^{-2} in the dark. These observations indicate a 24% enhancement in photocurrent as compared to the dark current. The SEM picture also reveals that the some of the surface of the substrate are devoid of composite particles that may cause some of the photoelectrons to be lost in these voids.

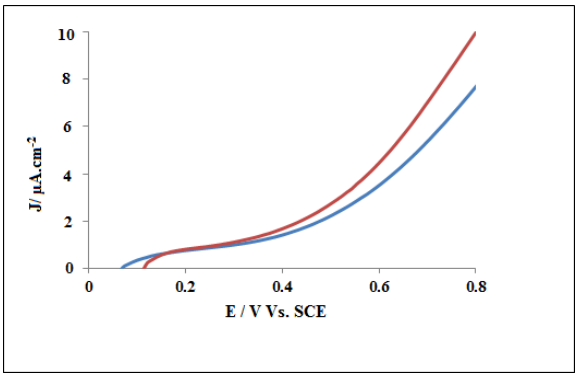

Fig. 6 PEC studies of Y_2CuO_4-5CuO in 0.01 M phosphate buffer solution (pH=9.2) under simulated sunlight and dark.

In summary the synthesised octa-nuclear Y-Cu complex provides an opportunity to fabricate Y_2CuO_4-5CuO composite thin films on glass substrate by AACVD at the relatively low temperature of 600 ^oC. The characterisation of the thin film by XRPD, SEM, EDX, Profilometer, UV-vis spectrophotometry provides information about crystallinity, surface morphology, particle shape and size, elemental composition, thickness of the film and indirect energy band gap of the composite to determine their technological applications.

4. Conclusions

We have developed a synthetic route for the synthesis of an octanuclear heterobimetallic Y-Cu complex **1** that was implemented to develop Y_2CuO_4-5CuO composite thin films under oxygen atmosphere from toluene solution by AACVD. The TG/DTG study of

the decomposition of complex **1** in oxygen and nitrogen ambient and FT-IR of the residues revealed dependence of decomposition mode of complex **1** on the environments. The Y_2CuO_4–5CuO composite thin film has well-defined, evenly distributed particles in the size range of 19-24 nm and offers optical band gap energy of 1.82 eV and a photocurrent density of 9.85 μAcm^{-2} at 0.80 V vs. SCE. All these observations indicate that the thin film is photoactive and generates holes and electrons that can be utilised for photoelectrochemical and solar energy applications.

Acknowledgements

MM acknowledges the High-Impact Research Grant No. UM.C/625/1/HIR/13, the UMRG Grant No. UM.TNC2/RC/261/1/1/RP007A/B-13AET and the FP033 2013A for funding this research.

Supplementary Information

The crystallographic data is also available from the Cambridge Crystallographic Data Centre (Fax: +44-1223-336-033; e-mail: deposit@ccdc.cam.ac.uk or http://www.ccdc.cam.ac.uk) as supplementary publication no. 950391

References

[1] D.L. Nelson, N.S. Whittingham, T.F. George (Eds.), Chemistry of High Temperature Superconductors, ACS Symposium Series 351, American Chemical Society, Washington, DC, 1987.

[2] D.R. Ulrich, *Chem. Eng. News,* 1990, **68**, 28.

[3] M.W. Rupich, B. Lagos and J.P. Hachey, *Appl. Phys. Lett.*, 1989, **55,** 2447.

[4] A. Grodzicki, I. Łakomska, P. Piszczek, I. Szyma´nska and E. Szłyk, *Coord. Chem. Rev.*, 2005, **249,** 2232.

[5] S. Reber, A. Hurrle, A. Eyer and G. Willeke, *Sol. Eng.* 2004, **77,** 865.

[6] A. Gicquel, K. Hassouni, F. Silva and J. Achard, *Curt. App. Phy.*, 2001, **1,** 479.

[7] S. G. Topping and V.K. Sarin, *Int. J. Ref. Met. Hard Mat.*, 2009, **27,** 498.

[8] T.A. Polleya, W.B. Cartera and D.B. Pokerb, *Thin Solid Films*, 1999, **357,** 132.

[9] R.G. Palgrave and I.P. Parkin, *J. Mat. Chem.*, 2004, **14,** 2864.

[10] J. Rodriguez-Castro, P. Dale, M.F. Mahon, K.C. Molloy and L.M. Peter, *Chem. Mater.*, 2007, **19,** 3219.

[11] J. Rodriguez-Castro, M.F. Mahon and K.C. Molloy, *Chem. Vap. Depos.*, 2006, **12,** 601.

[12] X. Hou and K.L. Choy, *Chem. Vap. Depos.*, 2006, **12,** 583.

[13] C.R. Crick and I.P. Parkin, *Thin Solid Films*, 2011, **519,** 2181.

[14] J.B. Biswal, N.V. Sawant and S.S. Garje, *Thin Solid Films*, 2010, **518,** 3164.

[15] S. Wang, *Inorg. Chem.*, 1991, **30,** 2252.

[16] A.P. Purdy and C.F. George, *Inorg. Chem.*, 1991, **30,** 1969.

[17] S. Wang, J. Z. Pang and M. J. Wagner, *Inorg. Chem.,* 1992, **31,** 5381.

[18] J. Zhang, L.G. Hubert-Pfalzgraf and D. Luneau, *Inorg. Chem. Commun.*, 2004, **7,** 979.

[19] S. Wang, S.T. Trepanier and M.J. Wagner, *Inorg. Chem.*, 1993, **32,** 833.

[20] C.P. Love, C.C. Torardi and C.J. Page, *Inorg. Chem.*, 1992, **31,** 1784.

[21] M. Hamid, M. Mazhar, Z. Arifin and K.C. Molloy, *Trans. Metal Chem.*, 2012, **37,** 241.

[22] M. Sultan, A.A. Tahir, M. Mazhar, M. Zeller and K.G. UpulWijayantha, *New J. Chem.*, 2012, **36,** 911.

[23] SAINT, Area detector integration software, Siemens Analytical Instruments Inc., Madison, WI, USA, 1995.

[24] G.M. Sheldrick, SADABS, Program for semi-empirical absorption correction, University of Göttingen, Göttingen, Germany, 1997.

[25] G.M. Sheldrick, *Acta Crystallogr.*, 2008, **A64**, 112.

[26] A. A. Tahir, K. C. Molloy, M. Mazhar, G. Kociok-Ko¨ hn, M. Hamid and S. Dastgir, *Inorg. Chem*., 2005, **44**, 9207.

[27] P. K. Larsen, R. Cuppens and G. A. C. M. Sprerings, *Ferroelectrics,* 1992, **128**.

[28] M. Shahid, M. Hamid, M. Mazhar, J. Akhtar, M. Zeller and A. D. Hunter, *Inorg. Chem. Comm.*, 2011, **14,** 288.

[29] M. Veith, M. Haas and V. Huch, *Chem. Mater.*, 2005, **17,** 95.

[30] G.B. Deacon and R.J. Phillips, *Coord. Chem. Rev.,* 1980, **33,** 227.

[31] B.H. Ye, X.Y. Li, I.D. Williams and X.M. Chen, *Inorg. Chem.*, 2002, **41,** 6426.

[32] N. Nawar and N.M. Hosny, *Trans. Met. Chem.,* 2000, **25,** 1.

[33] W. Suning, *Inorg. Chem.*, 1991, **30**, 2252.

[34] W. Suning, P. Zhen and M.J. Wagner, *Inorg. Chem.,*1992, **31**, 5381.

[35] A. B. Kuz'menko, D. V. Marel, P. J. M. van Bentum, E. A. Tishchenko, C. Presura, and A. A. Bush, *Phy. Rev. B,* **63**, 094303.

[36] Y. X. Zhang, M. Huang, F. Li and Z. Q. Wen, *Int. J. Electrochem. Sci.*, 2013, **8,** 8645.

[37] M. Aghazadeh, M. Ghaemi, A. N. Golikand, T. Yousefi and E. Jangju, *International Scholarly Research Network ISRN Ceramics,* 2011, 6.

[38] H. A. Silim, *Egypt. J. Solids*, 1991, **28,** 15.

[39] M. Mazhar, S. M. Hussain, F. Rabbani, G. Kociok-Köhn and K. C. Molloy, *Bull. Korean Chem. Soc.* 2006, **27**, 1572.

[40] F. Yakuphanoglu, S. Ilican, M. Caglar and Y. Caglar *J OPTOELECTRON ADV M*, 2007, **9**, 2180.

[41] D. Chauhan, V. R. Satsangi, S. Dass and R. Shrivastav, *Bull. Mater. Sci.*, 2006, **29**, 709.

[42] H. Kidowaki, T. Oku, T. Akiyama, A. Suzuki, B. Jeyadevan and J. Cuya, *Journal of Materials Science Research*, 2012, **1**.

[43] G.H. Li, L. Yang, Y.X. Jin and L.D. Zhang, *Thin Solid Films*, 2000, **368,** 163.

Graphical Abstract:

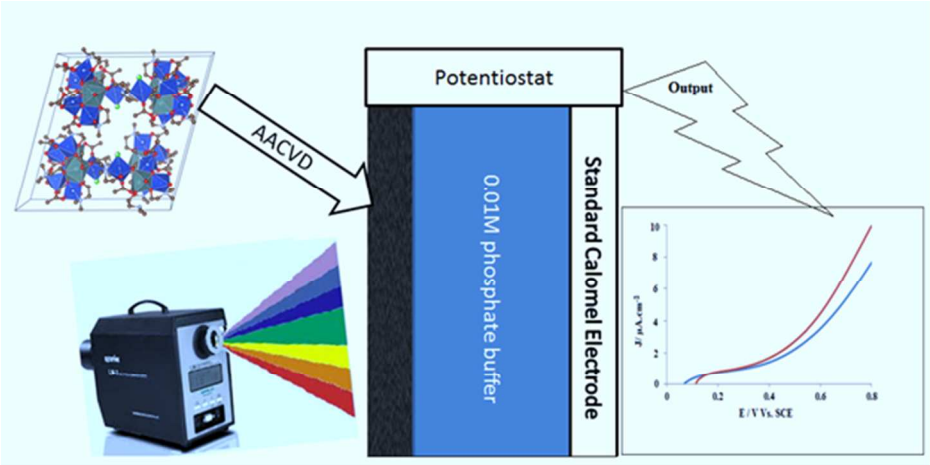

Y_2CuO_4-5CuO composite thin films having band gap of 1.82 eV and photocurrent density of 9.85 μA/cm^2 at 0.8 V have been deposited from a solution of precursor **1** by AACVD.